Supplemental Methods for Model-4

Dennis L. Chao
Institute for Disease Modeling

1 Model Description

The Institute for Disease Modeling cholera transmission model is based on a previous model described in (*1*). The model has been extended to allow it to be run over multiple years and to use rainfall data to drive cholera transmission. Many of the model parameters are summarized in Table 1, including those associated with the additions to the model. The model source code and data are available at: https://github.com/dlchao/cholera-model-haiti-2018.

The model is individual-based, so that each individual is explicitly represented in a synthetic population of Haiti. The synthetic population is spatially distributed on a 1km $\times$ 1km grid to represent the spatial extent of Haiti (Figure 1). For each grid cell, households are sampled from the appropriate Haitian department from the microcensus data from the Haitian Institute of Statistics and Informatics distributed by IPUMSi (*2*), based on 2003 census data. Each cell is populated with enough households to approximate the gridded 2015 population estimate from WorldPop (*3*). Specifically, we aggregate the 100m gridded estimate HTI_ppp_v2b_2015.tif (2015 estimate, not UN-adjusted) to a 1km $\times$ 1km grid to compute the target population of each cell. The ages of the individuals in the synthetic households is taken from the households sampled from the microcensus data, which reports ages to the nearest year. The age structure of the synthetic population should thus reflect the age structure of the Haitian population at the national, departmental, and household levels. The synthetic population has 10,911,656 people, 11.7% are under 5 years old and 212,230 (1.94%) of whom are 0 years old.

Individuals in each cell are aggregated into well-mixed communities of about 1,000 individuals, within which transmission occurs. When there are fewer than 1,500 individuals in a cell, they are considered to be a single community. Individuals can be susceptible, exposed, infectious, or recovered from cholera (Figure 2). Susceptible individuals can be infected either by exposure to infectious household members by exposure to contamination in the environment. Once infected, the individual is asymptomatic and non-infectious for a 1 to 5-day latent period. After the latent period, the individual has an 80% chance of becoming asymptomatically infected and a 20% chance of becoming symptomatically infected. Infectious individuals can both infect susceptible household members directly or shed *Vibrio* into the local environment associated with each community. We assume symptomatic infections shed 10$\times$ more than asymptomatic. Although symptomatic infections have been associated with orders of magnitude more shedding, we hypothesized that it would not be associated with proportionately higher transmission if symptomatic cholera incapacitates people (hampers mobility and social contacts). *Vibrio* in the environment decays at an exponential rate with a 14-day halflife. We had tested the model with shorter halflifes and found that the cholera frequently disappeared well before 2019, while values of 2 weeks or more allowed for persistence. If a community is on a river, infectious individuals shed into the river as well. Environmental *Vibrio* shed within the past day is *hyperinfectious* (*4*). The daily probability of infection from environmental *Vibrio* in the local community is:

$$\text{Probability of infection} = \beta \frac{(B + 2B_H)/N + B_R + 2B_{RH}}{\kappa + (B + 2B_H)/N + B_R + 2B_{RH}} \tag{1}$$

where B is the amount of contamination in the local environment, B_R is the amount of contamination in the local river (if the community is on a river), B_H is the amount of hyperinfectious *Vibrio* (shed within the last day) in the environment, B_{RH} is the amount of hyperinfectious *Vibrio* in the river, κ is the environmental half-saturation constant, and β is a scalar that can be adjusted to change the infectiousness of environmental *Vibrio*. Note that hyperinfectious *Vibrio* is assumed to be twice as infectious as non-hyperinfectious. After a 1 to 3-day infectious period, individuals recover and are immune to infection. In the current version of the model, immunity can wane. Each day, there is a small chance that recovered individuals become susceptible (simulates exponential distribution of protection from natural infection) so that the average duration of immunity is 8 years. This long duration of protection was necessary

to replicate the low levels of cholera for years after the initial outbreak, which we believe conferred protection to much of the population through infection. We found that when the immunity was shorter (3 or 5 years), the cholera epidemic resurged well before 2019. We added temporary immunity to the model for newborns. We draw a uniform random number from 0 to 364 days for each newborn to determine the length of full immunity. This is for two reasons: infants are at low risk of exposure (breastfeeding) and the synchronous fully susceptible birth cohort could trigger epidemics.

The model truncates very low probabilities of infection from the environmental reservoir to 0. Because the *Vibrio* level in the environmental reservoir decays exponentially, it never reaches 0 and the daily probability of infection from the reservoir should likewise approach but never reach 0. But because of the limitations of the random number generator (RNG) used, the daily probability of infection from the reservoir never dropped below 2^{-32}, which caused spontaneous resurgences of cholera long after apparent elimination occurred. In the model, a random event (such as infection) occurs if the value drawn from the random number generator is less than the probability of the event in question. The model uses GSL's 32-bit random number generator (GNU Scientific Library version 2.5, https://www.gnu.org/software/gsl/doc/html/index.html), which generates pseudorandom numbers in the range of 0 to 4294967295 then converts these integers to doubles by dividing by 4294967296. Since the RNG returns 0 with a probability of $1/2^{32}$, then the lowest probability our code can handle is 2^{-32}. We addressed this issue by assuming no infection occurs if the daily infection probability from the reservoir is below 2^{-32}.

Transmission of disease across communities can occur in several ways: commuting to work, traveling along highways, sporadic long-distance travel, and rivers, which are described in more detail in (*1*). Working-age individuals spend a portion of their time in communities some distance away according to a power law. They can therefore become exposed to cholera at these work destinations or shed cholera in them. Because the model now includes age, we now specify that 60% of individuals 15 years old and older "commute" to work, based on Haiti's employment-to-population ratio reported at https://fred.stlouisfed.org/series/SLEMPTOTLSPZSHTI. Major highways are included in the model. Individuals living next to a highway have a small chance each day of swapping positions with another individual along the road network. This simulations the travel of susceptible of infectious individuals on longer trips while keeping the population size of their respective communities constant. Even less frequently, random individuals

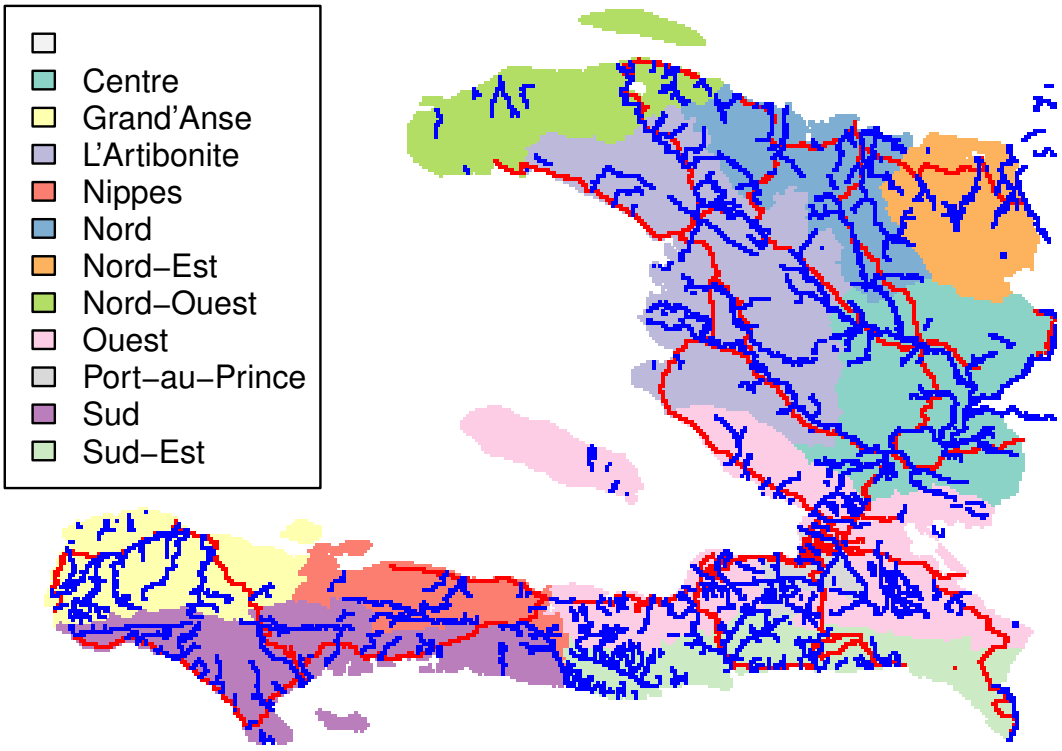

Figure 1: Map of departments and major features of Haiti. Rivers are in dark blue, highways in dark red, and the population associated with each department is in the color indicated by the legend.

from across the country can be swapped, which mimics sporadic long-range travel that is not dictated by the road network. The locations and directionality of rivers are included in the model. Vibrio shed into rivers travels downstream each day, potentially infecting individuals in downstream communities. Highway and river locations were obtained from OpenStreetMap (*5*).

The new version of the model ages the population for simulating multi-year epidemics. We age the population on March 15 of every year, which has been reported to be the "low season" for cholera (*6*). Within the model individuals are not explicitly aged, but instead we copy the immune status (but not active infections) from individuals one year younger in the same "community" (about 1000 individuals or less), as we did in a previously described dengue model (*7*). Newborns (age 0 years) are set to be unexposed. Household structures and ages are kept constant. We found that if we drew from the same 1kmx1km grid instead of community, Port-au-Prince and Nord would experience out-of-season outbreaks in April. These regions contain the most densely populated part of Haiti, and might sustain cholera through the dry season.

We assume that environmental shedding by infectious people is dependent on a department's rainfall that day. We obtain rainfall by computing the average rainfall that falls across the extent of each department each day according to the STAR Satellite Rainfall Estimates from 2010 through 2018 (https://www.star.nesdis.noaa.gov/smcd/emb/ff/HEsouthAmerica.php). When simulating years after 2018, we draw from rainfall data in one-year blocks (January 1 through December 31) from 2010 through 2018 excluding 2013, which had a long gap in the data. We used the rainfall estimates for Ouest department for the population of Port-au-Prince. If rainfall data are missing, we assume there is no rain that day. For modeling simplicity, we assume all years are 365 days, so we skip leap days in the weather data. Daily rainfall ranged form 0 to over 330mm of rain, and there is generally more rain in the south than in the north (Figure 3). The amount of *Vibrio cholerae* shed into the environment is multiplied by one of 5 scalars based on the day's rainfall. Environmental shedding is lowest on days with no rainfall (about 55% of days depending on the department), and higher when there is more rainfall, as defined by four categories: $<$ 1mm (about 16% of all days), $<$ 10mm, $<$ 50mm, or $\geq$ 50mm rainfall in a day (Figure 3A).

As in the previously published version of the model, vaccine can protect against infection (VE_S), illness given infection (VE_P), and infectiousness (VE_I). We generally assign either VE_S or VE_P to be > 0 and the other parameters to 0. In the previous version of the model we had protection from vaccine increase from 0 to full efficacy over a period of two weeks in order to simulate a dosing schedule. We now assume that vaccine is effective upon administration, since timing will be less critical when vaccine is administered years after the epidemic peak in 2010–2011. We also only model vaccination with both doses of cholera vaccine, so we do not model those who only get one dose. We

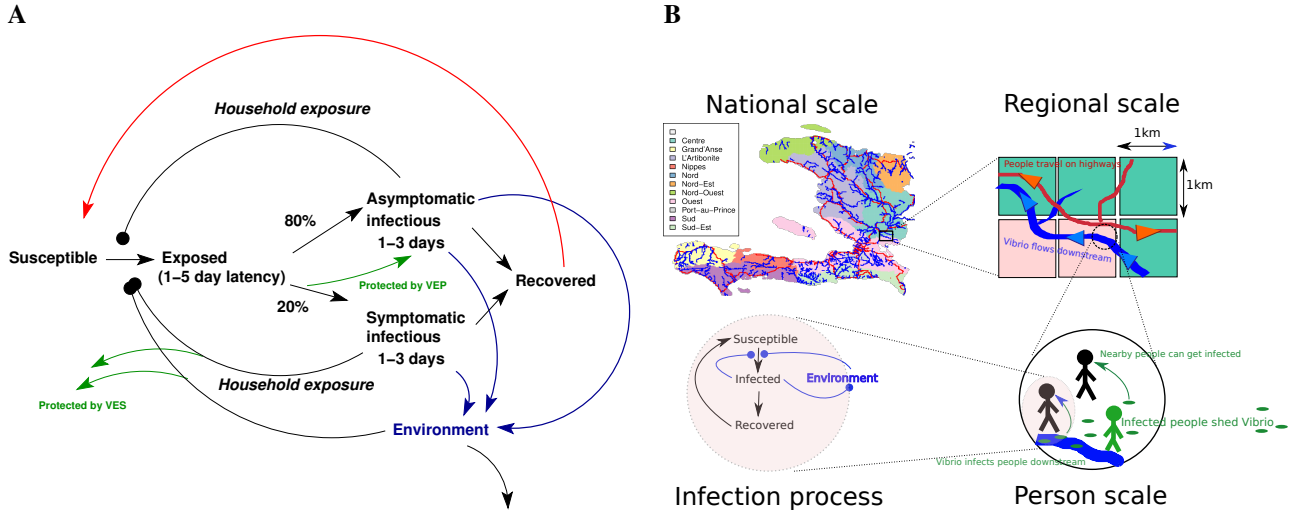

Figure 2: Model structure. A) Model compartmental diagram, modified from reference (*1*). The new features include waning of immunity (red arrow) and the seasonally-driven environmental shedding (blue arrows). For this project, we explore the effect of rainfall on shedding (blue arrows), the impact of vaccination (green dashed arrows), and infectiousness of V cholerae in the environment (black arrow from "Environment" to the Susceptible–Exposed transition arrow). B) Model overview diagram.

assume that vaccine is only 46.9% as protective among children under 5 years old than those older (*8*). We believe that this reduced protection depends on the age at vaccination, not age at exposure (*9*). We assume that vaccine protection either does not wane or wanes linearly over time to approximate the log-linear waning scenarios (Figure 4).

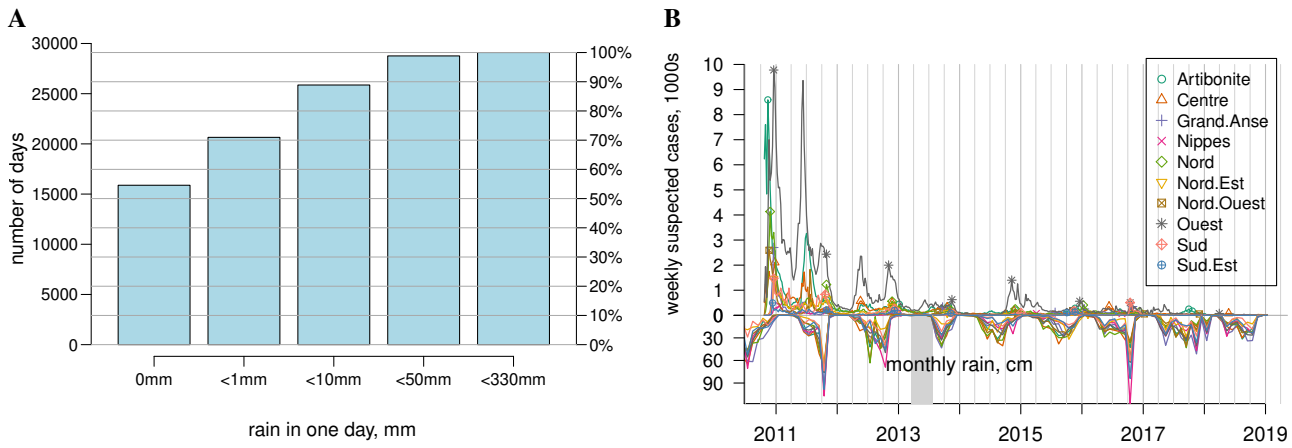

Figure 3: Rainfall data. A) Amount of rainfall per day (averaged over departments). Each point on the y-axis is actually a "department–day", so the total number of data points is the number of days from 2010 to 2017 times 10. The highest amount of rainfall a department had in one day was 326.5mm. The bar on the right ("<330mm) includes all department–days of data. B) Weekly suspected cholera cases and monthly rainfall. Monthly rainfall by department is plotted below the x-axis. The gray bar indicates a 127-day gap in the satellite data from 2013.

Table 1: Subset of model parameters. Some parameter values were taken from the previously published version of the model and further explanation can be found in (*1*).

parameter	default (range tested)	source/notes
incubation period	1–5 days	(*1, 10*)
infectious period	1–3 days	(*11, 12*)
duration of immunity after infection	8 years	
fraction symptomatic	20%	(*1*)
asymptomatic/symptomatic shedding ratio	10%	(*1*)
maximum daily probability of infection (β)	0.1 (0.05–0.35)	parameter sweeps A and B
environmental half saturation (κ)	0.2 (0.1–1.2)	parameter sweep A
shedding with low rain	1.0	reference
shedding with no rain	0.3 (0.2–0.8)	parameter sweeps B and C
shedding with heavy rain	6 (2–10)	parameter sweep C
decay of *V cholerae* in the environment	1/14 days^{-1}	
hyperinfectious *V cholerae* infectiousness	2×	
amount shed into river (relative to environment)	1%	

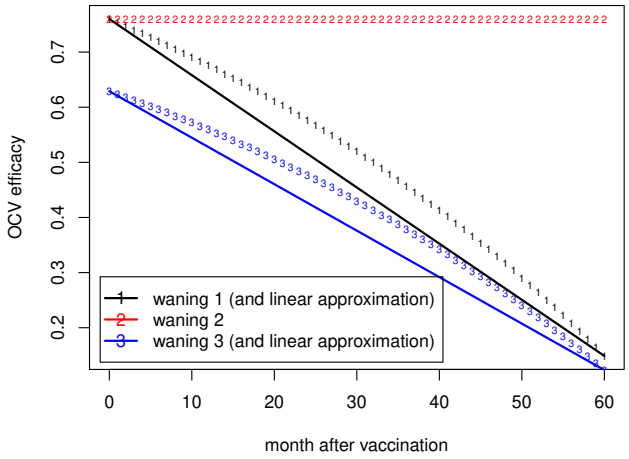

Figure 4: Vaccine efficacy waning scenarios. The consortium proposed 1-VE to decay at a log-linear rate, with a linear rescaling of efficacy for VE waning scenario 1 (plotted as numbers). The model approximates this as linear decay (solid lines). VE continues to decline until efficacy is 0.

2 Model Selection and Fitting/Calibration

We qualitatively fit the cholera transmission model so that the weekly symptomatic cholera cases had a few of the key features as the nationwide weekly suspected cases reported by MSPP from 2010 through 2018 (Figure 5) (*13*). Because the reporting rate of cholera likely differed across departments (*14*) and over time, we felt that matching the timing and relative magnitude of peaks would be more robust to these variations than attempting to quantitatively fit the data as a time series assuming a fixed reporting rate. We focused on producing the two large peaks in the first year of the epidemic (from late 2010 through the fall of 2011), the regular peaks coinciding with the rainfall around October–November each year, and the persistence of cholera through at least January 2019. Because of the computational cost of running the model, we performed a limited exploration of parameter space and used parameter value estimates from the earlier publication (*1*) when possible.

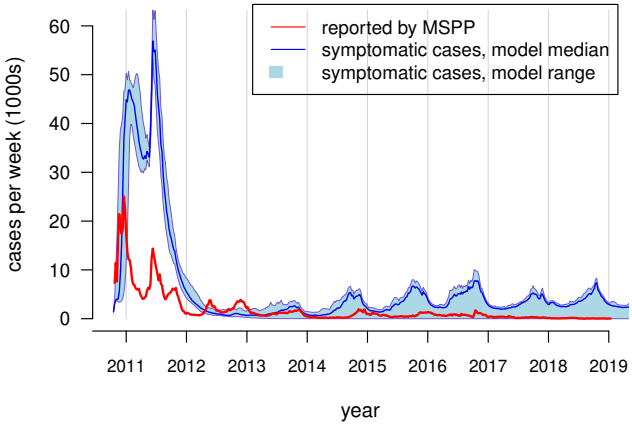

Figure 5: Model fit to MSPP data. The red line indicates the number of suspected cholera cases reported by MSPP per week. The blue line indicates the median number of symptomatic cholera cases per week, while the light blue region spans the minimum and maximum number from 30 stochastic model runs.

We performed three "sweeps" of parameters, varying only two free parameters per sweep. For the first parameter sweep ("A", see Figure 6), we varied κ and β (see Equation 1). These are the two parameters that govern overall transmissibility of cholera. In parameter sweep B, we fixed κ and varied β and the relative amount of shedding on days with no rainfall (Figure 6). We believe this parameter combination would determine the persistence of cholera during the dry seasons in Haiti. In parameter sweep C, we fixed κ and β and varied the relative amount of shedding on days with no rainfall and days with the highest levels of rainfall (Figure 6). We believe this parameter combination determines the duration and height of seasonal cholera peaks.

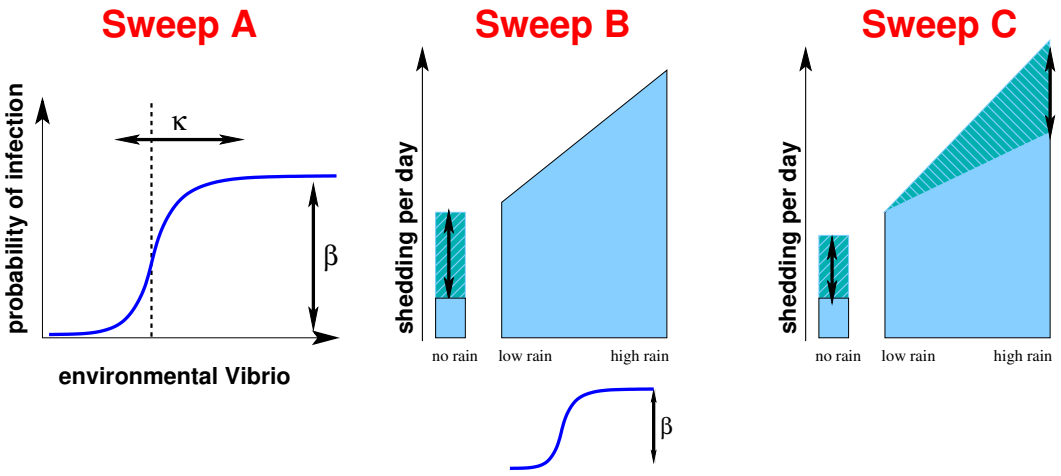

Figure 6: Diagram of the three parameter sweeps. In "sweep A", we vary κ and β. In "sweep B", we vary the amount of shedding when there is no rain and the amount of shedding when there is heavy rain. The amount shed when there is low rain is fixed and the intermediate levels are linearly interpolated. In "sweep C", we vary the amount of shedding when there is no rain and β.

3 Assessment of Model Fit

Since the earlier published version of the model, we have made several changes that affected our choice of parameter values. In (*1*), those infected with cholera were infectious from one to two weeks. Although infected people may in reality shed for over a week, we believe that a shorter period is more appropriate for the purposes of modeling transmission. (*12*) used historical data to estimate the serial interval to be 3.7 days, and this seems consistent with observations in Bangladesh (*11*). Since we assume the latent period to be about 1.5 days (range of 1 to 5 days), then the infectious period should be 2 days in our model to match an approximately 3.5 day serial interval. We decided to make individuals infectious for 1 to 3 days (uniform distribution). Reducing the infectious period necessitated a cascade of other parameter changes. We also reduced the relative infectiousness of hyperinfectious *Vibrio*. Originally, we assumed that environmental *Vibrio* was 100$\times$ more infectious on the first day relative to subsequent days (*4*). This effectively creates a "person-to-person" cholera transmission that is 100$\times$ stronger than the "environmental" transmission, which would basically be an SIRS model with a short serial interval and negligible environmental component. To allow the environmental component to play a more important role in transmission, we decreased the infectiousness of hyperinfectious *Vibrio* to be only 2$\times$ as infectious. After making all of these changes, we ran several 2-parameter sweeps to find appropriate values for the parameters introduced in this version of the model.

For parameter sweep A, we found that setting κ to 0.1-0.2 and β to 0.1 generated epidemic curves with two major peaks during the first year of the epidemic. Higher values of κ were often associated with years in which there were no seasonal peaks, and higher values of β caused cholera to spread throughout the country to rapidly so that there was only a single massive peak during the first year (Figure 7). When $\kappa = 0.2$ and $\beta = 0.1$, there were about 2,000,000 cases of cholera by the end of 2011 (Figure 8). In the MSPP reports (*13*), there were about 500,000 suspected cases by this point, implying a reporting rate of about 25%. Our model considers only "asymptomatic" and "symptomatic" cases and ignores the spectrum of illness that actually occurs, so it is difficult to interpret this estimated reporting rate. The MSPP also reports the estimated number of suspected cases who were under 5 years old and the number $\geq$5 years. In the model, about 10% of cases are under 5 when the epidemic starts, but this fraction climbs to about 20% within four years or less 9. This is because initially the entire population is fully susceptible to infection so cholera strikes all age groups equally, but as the epidemic progresses the population exposed to cholera ages and susceptible birth cohorts are introduced each year.

In parameter sweep B, we fixed κ and varied β and the relative amount of shedding on days with no rainfall (Figure 6). We found that when there was a high amount of shedding when there was no rainfall (e.g., shedding was reduced by a factor of 0.5 compared to days with minimal rainfall), the seasonal peaks of cholera started to flatten, but when shedding was too low during periods with no rain, cholera would often disappear after the second or third year of the epidemic (Figure 10). We found that shedding 0.3 on rainless days compared to days with minimal rain produced plausible seasonal peaks.

In parameter sweep C, we fixed κ and β and varied the relative amount of shedding on days with no rainfall and days with the highest levels of rainfall (Figure 6). We assume a linear relationship between rainfall and shedding to the environment, so shedding at intermediate levels of rainfall is interpolated between 1.0 (the base level of shedding when there is minimal but $>$0 rainfall) and the level of shedding at the highest levels of rainfall. When the relative shedding at the highest levels of rainfall was too low (e.g., only twice as high as at minimal rainfall), the seasonal peaks were too long. We suspect that there is more cholera transmission during the heavier rains from September to November than during the lighter rains from March through May. The seasonal peaks looked more realistic at higher levels of shedding with high rains (six or ten times as much shedding), but it was difficult to pick an optimal value (Figure 7).

To project the effectiveness of cholera vaccination, we simulated cholera transmission through 2029. For simulating transmission from 2010 through 2018, we used rainfall data from the appropriate years, but we re-used these data to simulate rainfall from 2019 onward. To do this, we drew random permutations of the years with sufficient rainfall data (2010 through 2018 except for 2013), then generated rainfall time series by concatenating data from these years (daily data from January 1 through December 31). We generated 30 rainfall time series, so that we could run the model 30 times. Thus, the model runs include both stochastic effects for all years and rainfall differences from 2019 onward. We also filled in the gap in data from April 1 2013 to July 25 2013 with data from randomly selected years. Because each run used different rainfall data after 2018, the model results had more variation after 2018 (Figure 12). Prediction of major events like hurricanes would improve forecasting of cholera transmission and the impact of vaccination (*15*).

We found it difficult to maintain cholera transmission at low levels, and we deliberately chose parameters to ensure persistence of cholera through 2019. We therefore consider our model fit to produce an overestimate of transmission,

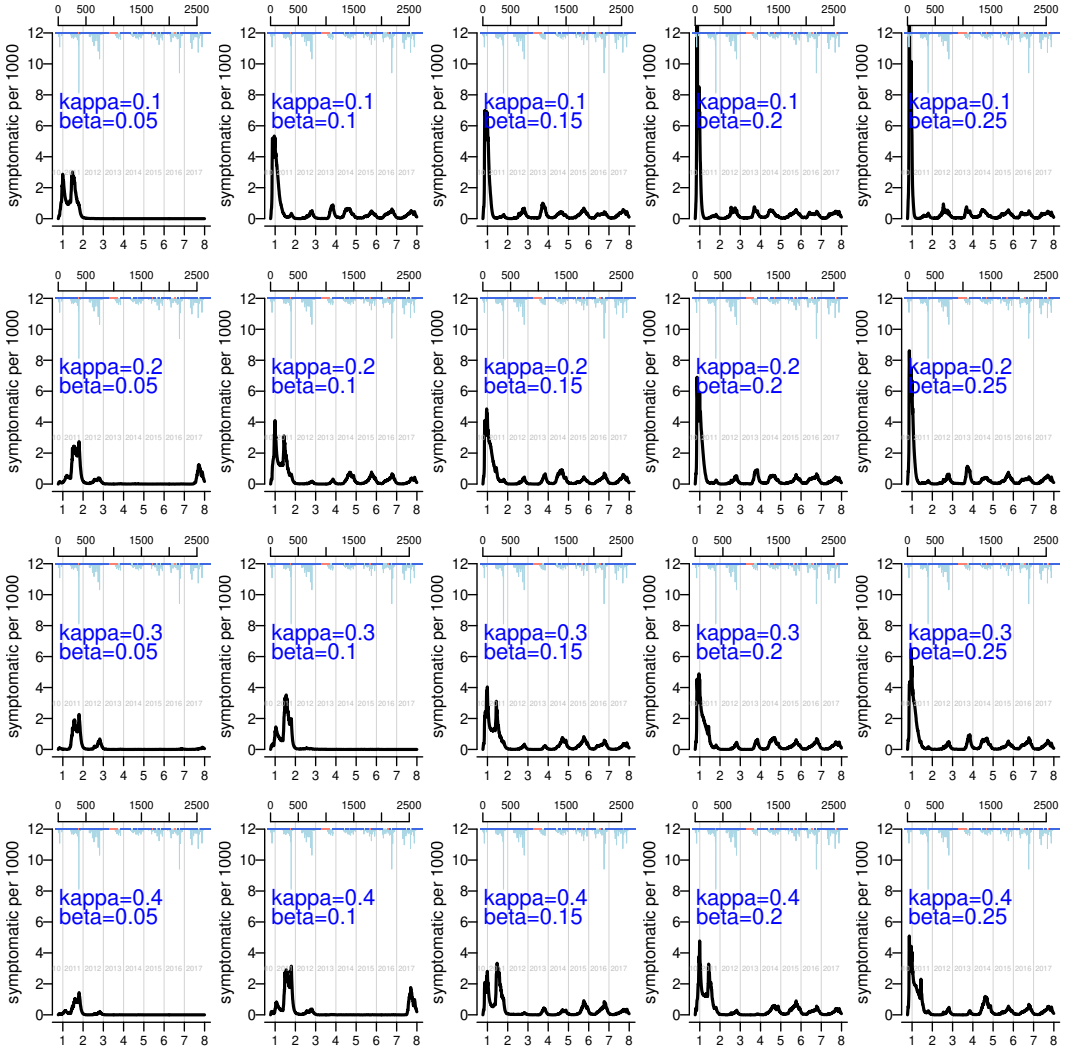

Figure 7: National symptomatic cholera prevalence in parameter sweep "A". The bottom x-axis has tick marks on January 1 of each year, and the top x-axis has the number of days of simulation. Year "1", the first full year of the simulations, corresponds to 2011. κ and β were varied. Shedding when there is no rain was 0.3 times shedding when there is minimal rain, and shedding is 6 times higher when there is heavy rain.

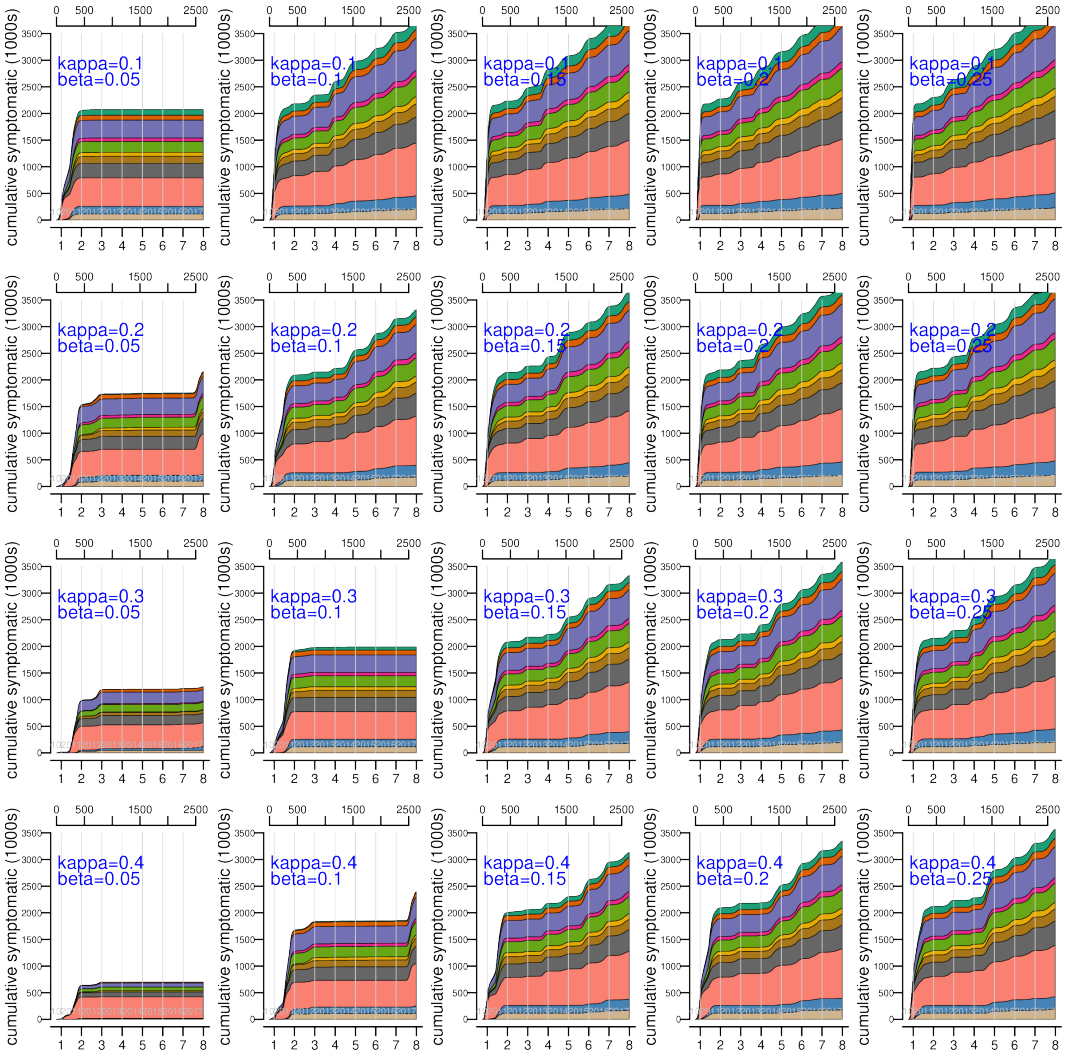

Figure 8: Cumulative symptomatic incidence in parameter sweep “A”. Cumulative incidence of symptomatic cholera for each department is plotted as different colors.

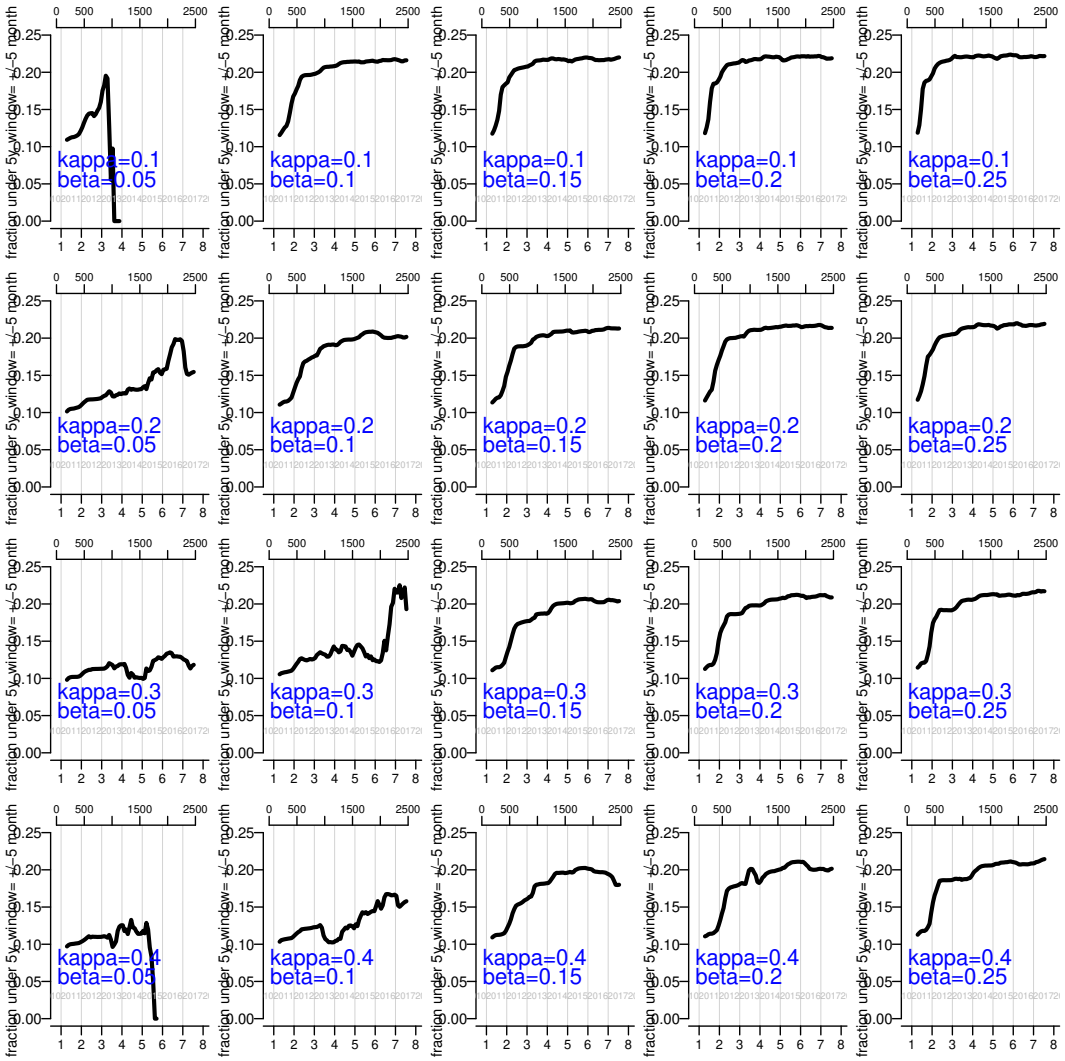

Figure 9: Proportion of symptomatic cases under 5 years old in parameter sweep “A”. The proportion was computed over an 11-month moving window (using data from 5 months before to 5 months after to plot each month’s proportion
.

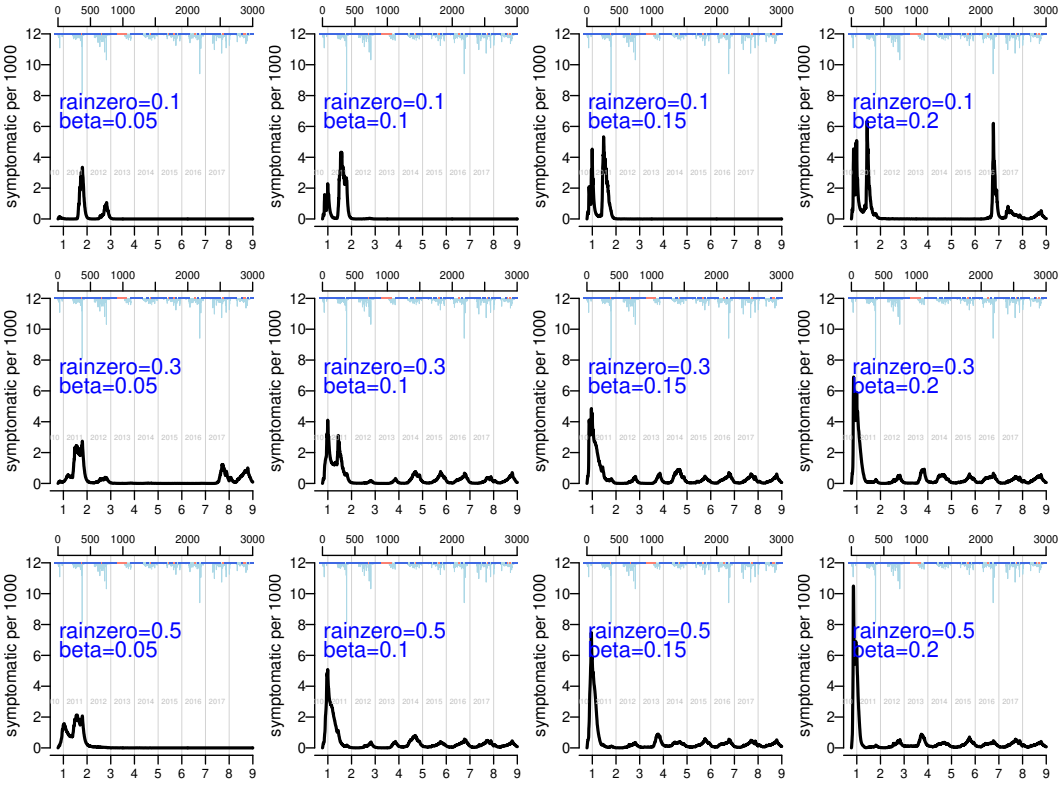

Figure 10: Symptomatic prevalence in a parameter sweep of beta and rainzero (sweep "B"). Cumulative incidence of symptomatic cholera for each department is plotted. The shedding when there is minimal rain is 1.0 and heavy rain is 6.0. Shedding when there is no rain (from top to bottom row: 0.1,0.3,0.5), and beta is varied from 0.1 to 0.25 (left to right: 0.1,0.15,0.2,0.25,0.3,0.35).

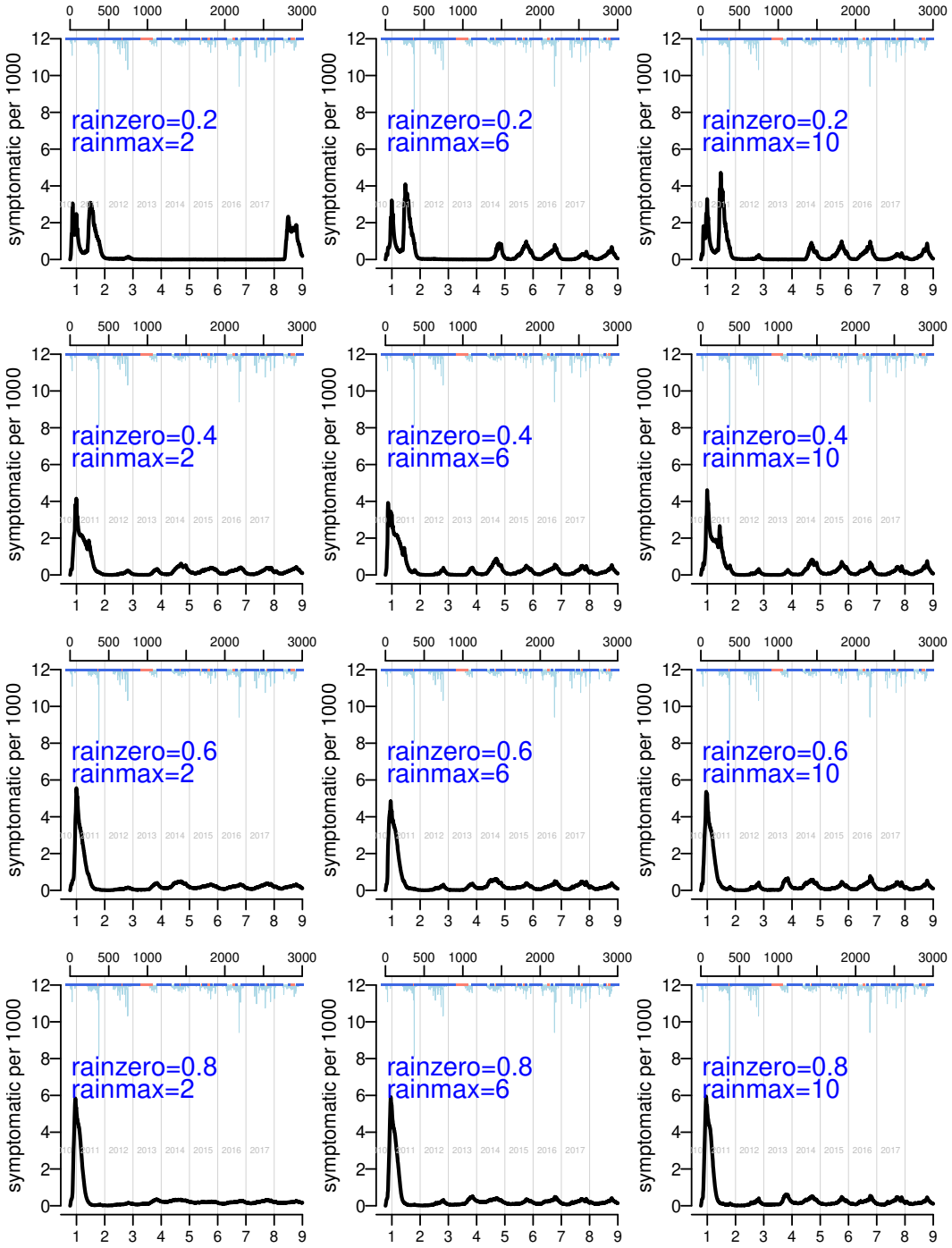

Figure 11: Symptomatic cholera prevalence in parameter sweep of rainfall parameters (sweep "C"). Prevalence of symptomatic cholera for each department is plotted. The bottom x-axis has tick marks on January 1 of each year, and the top x-axis has the number of days of simulation. The shedding when there is minimal rain is 1.0. Shedding when there is no rain (from top to bottom row: 0.2,0.4,0.6,0.8) and when there is heavy rain (from left to right column: 2, 6, 10) are simulated.

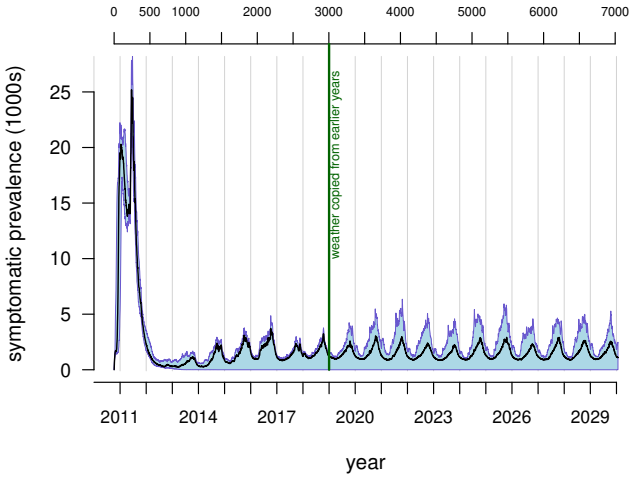

Figure 12: The results of 30 runs without interventions. Starting in January 2019, rainfall data is drawn from previous years. The blue region shows the minimum and maximum prevalence of symptomatic cholera across stochastic runs, and the black line shows the median. Rain data from 2010 to 2018 is used, and rain for each year after 2018 is copied from randomly selected years (excluding 2013).

particularly after the initial epidemic peaks. Our model assumes that transmissibility of cholera, behavior of people, and the population size does not change over time. Given these constraints, the incidence of cholera slowly increases over time after the first waves in the model, since the population-level immunity from the initial epidemic disappears over time by waning immunity and population turnover. We also assume that there is no long-term environmental reservoir that would allow cholera to persist in Haiti.

4 Simulation of Vaccination Campaigns

We simulated rollout of vaccine by department. We assumed that vaccinated people were protected from infection but not against showing symptoms after getting infected ($VE_S > 0$ and $VE_P = 0$). We vaccinate approximately the same number of people each day from the start to the end date of the rollout. After vaccination is scheduled to start, a fixed amount of vaccine is added to the supply each day and cells (1kmx1km areas) within the desired department are chosen randomly for vaccination until the available vaccines are depleted. Small amounts of vaccine that are not used are carried forward to the next day. Cells are only vaccinated when there is sufficient vaccine to cover them at the desired level – those that are too large may be selected again later. Within the department of Ouest, we treat the communes of Port-au-Prince as a separate department for bookkeeping purposes. When we vaccinate Ouest, we first vaccinate the Port-au-Prince communes. We define "Port-au-Prince" to be the communes of Port-au-Prince, Delmas, Carrefour, and Pétion-Ville (about 2.6 million people). IHSI also includes the communes of Cite Soleil and Tabarre in Port-au-Prince, but they are not in the GADM shapefile we used.

We simulate four vaccination scenarios: full country in 2 years (scenario #1), two departments in 2 years (Centre and L'Artibonite) (scenario #2), full country in 5 years (scenario #3), and three departments in 2 years (Centre, L'Artibonite, and Ouest) (scenario #4). All rollouts begin on January 12, 2019, and departments are vaccinated in order of highest to lowest reported incidence in 2014 (Centre, L'Artibonite, Ouest, Nord-Ouest, Nord, Sud, Nippes, Nord-Est, Sud-Est, and Grand Anse). In these scenarios, 10,463, 2,348, 4,185, and 6,184 people are (fully) vaccinated per day, respectively, which covers 70% of the population. See Figure 13 for the number of individuals vaccinated in these four scenarios. The model does not accommodate "partially-vaccinated" people (i.e., everyone gets both doses of vaccine), so we do not consider 1-dose coverage in a vaccination campaign. Population-level vaccine coverage drops by nearly 2% per year because of births and deaths.

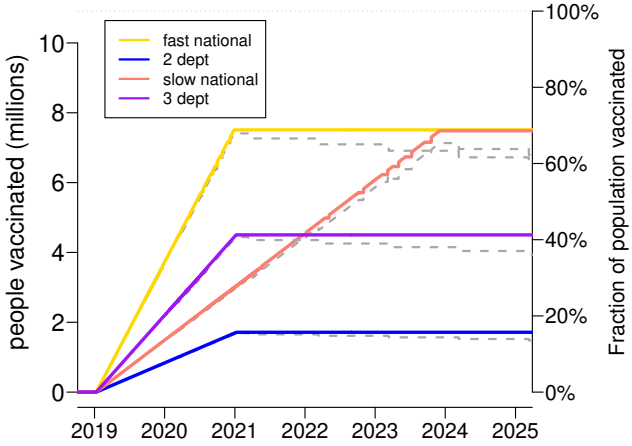

Figure 13: Number of individuals vaccinated in the simulations. Solid lines plot the cumulative number of people vaccinated for the four vaccination scenarios. Dashed gray lines indicate the number of living vaccinated people in the population, which declines as new individuals are born and others die. The left y-axis is scaled to the number of people vaccinated while the right y-axis is scaled to the fraction of Haiti's population that is vaccinated. All vaccinees receive both doses of OCV – no one is vaccinated with only one dose.

5 Calculating Elimination Measures

We define elimination to be the absence of any new cholera infections for one year. The time of elimination is the first day of a 365-day window with no new cholera infections (although there may be more infections one year after that), and the "time to elimination" is the number of days from January 12 2019 to the time of elimination. We found that in some runs, cholera spontaneously disappeared before vaccination started. We did not include these runs when computing the probability of elimination. We define the probability of elimination to be the fraction of runs have elimination among those that do *not* have elimination before the intervention starts. Resurgence is defined as seeing a new cholera infection after apparent elimination. We have an alternative definition of elimination that uses a threshold (T), where elimination is defined as when there are $< T$ (rather than < 1) new infections during a one-year window, and resurgence is defined as seeing T new cholera infections within any 365-day window after apparent elimination.

We did not observe a resurgence of cases after infections are not observed for one year (Figure 14). In theory, the aquatic reservoir could spark a new epidemic after such a long absence of cases but this is very unlikely because the amount of *Vibrio* in the reservoir decays exponentially and no external contamination or infected people are introduced. For the scenarios tested, once the number of infections drops below 1000 per year, resurgence was not observed (Figure 14). If there are 1000–9999 cases in a one-year window, resurgence could occur. When vaccine efficacy does not wane, elimination frequently occurs with the 2-year nationwide rollout with 70% coverage (Figure 15). In these runs, elimination generally occurs within three or four years of the start of vaccine rollout, so we would expect similar probability of elimination if the vaccine maintains high efficacy for 4 years.

Variation among runs for a single scenario comes from a combination of stochastic effects (different random number generator seeds) and the different random draws that determine rainfall after December 2018 and during the spring of 2013 with missing rainfall data.

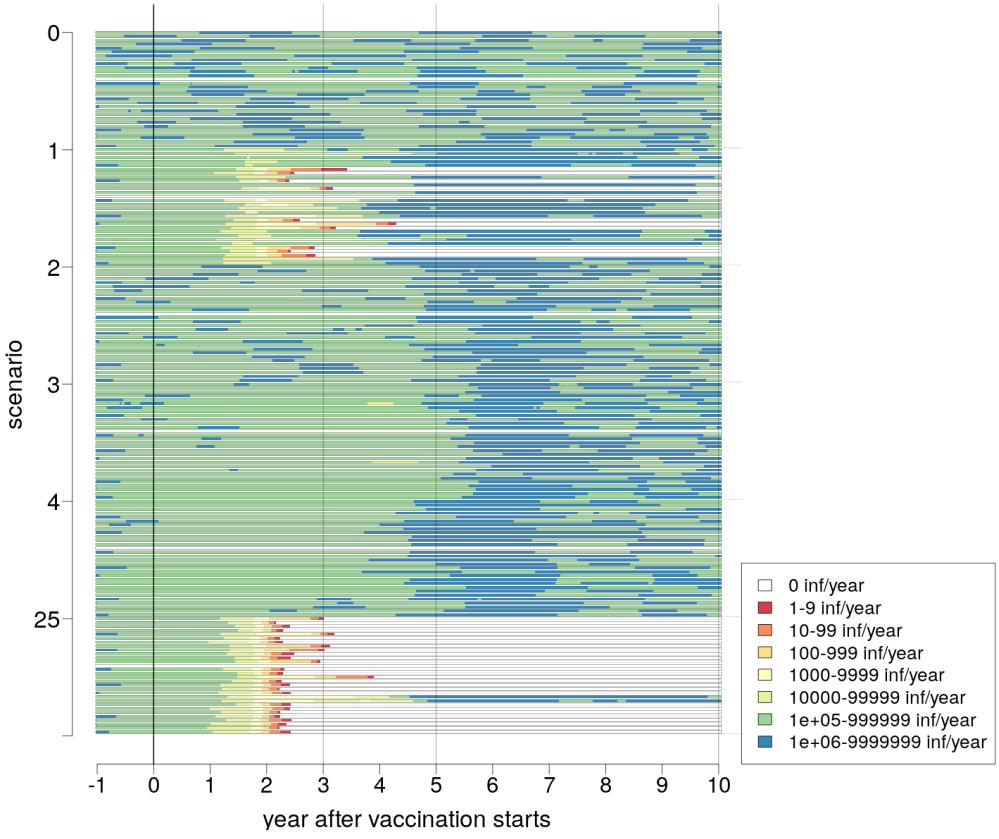

Figure 14: Numbers of infections over time for six vaccination scenarios. Each horizontal line represents the output from a single stochastic run. Six scenarios were chosen: 0) no vaccination, 1) vaccination of the whole country over 2 years (70% vaccine coverage), 2) vaccination of 2 departments over 2 years, 3) vaccination of the whole country over 5 years, 4) vaccination of 3 departments over 2 years, and 25) vaccination of the whole country over 2 years with high coverage (95% coverage). The runs for each scenario is depicted as a stack of 30 horizontal lines. For each day of the year, the number of cholera infections that occur over the next 365 days is indicated by color. For example, regions in red indicate days for which there are only 1 to 9 infections over the next 365 days in the model run, while green indicates 100,000 to 999,999 infections. White dots indicate that no new infections occur within 365 days, the strictest definition of "elimination".

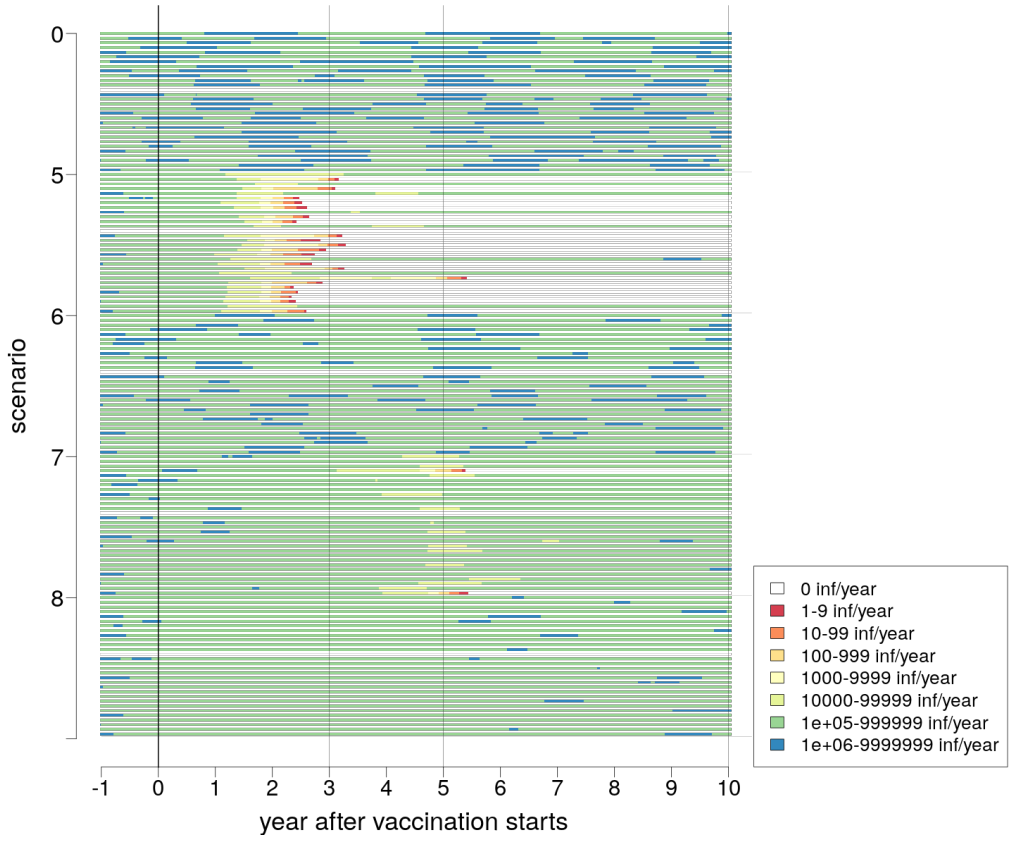

Figure 15: Numbers of infections over time for five vaccination scenarios with no vaccine efficacy waning. Each horizontal line represents the output from a single stochastic run. Five scenarios were chosen: 0) no vaccination, 5) vaccination of the whole country over 2 years, 6) vaccination of 2 departments over 2 years, 7) vaccination of the whole country over 5 years, and 8) vaccination of 3 departments over 2 years. The runs for each scenario is depicted as a stack of 30 horizontal lines. For each day of the year, the number of cholera infections that occur over the next 365 days is indicated by color. For example, regions in red indicate days for which there are only 1 to 9 infections over the next 365 days in the model run, while green indicates 100,000 to 999,999 infections. White dots indicate that no new infections occur within 365 days, the strictest definition of "elimination". In these scenarios, vaccine efficacy does not decline over time.

References

1. D. L. Chao, M. E. Halloran, I. M. Longini, Jr., *Proc Natl Acad Sci U S A* **108**, 7081 (2011).
2. Minnesota Population Center, Integrated public use microdata series, international, Available at `https://international.ipums.org/international/` (2019).
3. A. Sorichetta, *et al.*, *Sci Data* **2**, 150045 (2015).
4. D. M. Hartley, J. G. Morris, Jr., D. L. Smith, *PLoS Med* **3**, e7 (2006).
5. OpenStreetMap contributors, Planet dump retrieved from https://planet.osm.org , `https://www.openstreetmap.org` (2019).
6. S. Rebaudet, *et al.*, *PLoS Curr* **5** (2013).
7. D. L. Chao, S. B. Halstead, M. E. Halloran, I. M. Longini, Jr., *PLoS Negl Trop Dis* **6**, e1876 (2012).
8. Q. Bi, *et al.*, *Lancet Infect Dis* **17**, 1080 (2017).
9. Y. Fong, *et al.*, *BMC Infect Dis* **18**, 84 (2018).
10. D. A. Sack, R. B. Sack, G. B. Nair, A. K. Siddique, *Lancet* **363**, 223 (2004).
11. A. A. Weil, *et al.*, *Clin Infect Dis* **49**, 1473 (2009).
12. M. Phelps, *et al.*, *J Infect Dis* **217**, 641 (2018).
13. Ministère de la Santé Publique et de la Population, Profil statistique cholera, http://mspp.gouv.ht/newsite/.
14. J. R. Andrews, S. Basu, *The Lancet* **377**, 1248 (2011).
15. E. Hulland, *et al.*, *Am J Trop Med Hyg* **100**, 368 (2019).